PCCP

PAPER

View Article Online
View Journal

Cite this: DOI: 10.1039/d3cp01408h

Water adsorption lifts the (2 × 1) reconstruction of calcite(104)†

Jonas Heggemann,[a] Simon Aeschlimann,[b] Tobias Dickbreder,[b] Yashasvi S. Ranawat,[c] Ralf Bechstein,[b] Angelika Kühnle,[b] Adam S. Foster *[cd] and Philipp Rahe *[a]

Received 28th March 2023,
Accepted 26th June 2023

DOI: 10.1039/d3cp01408h

rsc.li/pccp

The adsorption of water on calcite(104) is investigated in ultra-high vacuum by density functional theory (DFT) and non-contact atomic force microscopy (NC-AFM) in the coverage regime of up to one monolayer (ML). DFT calculations reveal a clear preference for water to adsorb on the bulk-like carbonate group rows of the (2 × 1) reconstructed surface. Additionally, an apparent water attraction due to carbonate group reorientation suggest island formation for water adsorbed on the reconstructed carbonate group rows. Experimentally, water is found to exclusively occupy specific positions within the (2 × 1) unit cell up to 0.5 ML, to form islands at coverage between 0.5 and 1 ML, and to express a (1 × 1) structure at coverage of a full monolayer.

Introduction

The interaction between water and mineral surfaces is of broad importance from the planetary down to the atomic level.[1] In particular, the mineral calcite, the prevalent modification of calcium carbonate ($CaCO_3$), is of key relevance in many processes, including the global cycling of elements,[2] controlling geochemical dissolution-precipitation processes,[3] and as an essential constituent of biominerals in living organisms.[4]

Very recently, it has been established[5] by a combination of high-resolution non-contact atomic force microscopy (NC-AFM) imaging at 5 K and density functional theory (DFT) calculations that the pristine (104) surface, the most stable cleavage plane of calcite,[6] bears a (2 × 1) reconstruction and belongs to the planar space group *pg*. The (2 × 1) reconstruction of calcite(104) is mainly expressed by a rotation of every second carbonate (CO_3) group along the [010] direction, while the *pg* space group contains a glide plane reflection as the symmetry element. These properties lead to the presence of two different carbonate group rows on the surface: an unreconstructed bulk-like (S) and a reconstructed (R) row, both running along the [42$\bar{1}$] surface direction (see also Fig. 1(a)). Additionally, smaller shifts at the two calcium (Ca) ion sites P and Q lead to a mostly vertical difference between these sites that appears experimentally as a chequerboard-like pattern. Considering previous experimental reports of (2 × 1) effects at 300 K,[7–9] this reconstruction is consequently present across a large temperature range under vacuum conditions. Combined with the finding of two different adsorption sites of carbon monoxide molecules at a temperature of 5 K,[5] it is clear that the adsorption of further molecules on calcite(104) should be studied in light of the (2 × 1) surface reconstruction. In particular, the observation of a (2 × 1) reconstruction is so far conflicting with the measurement of (1 × 1) water structures in liquid-based force measurements.[10]

Here, we use both DFT and NC-AFM for describing a lifting of the surface reconstruction that is observed at water coverage of more than 0.5 monolayer (ML) on calcite(104). NC-AFM images acquired at 140 K show that water exclusively occupies one half of each (2 × 1) unit cell up to a coverage of 0.5 ML, forms islands at coverage between 0.5 ML and 1 ML, and follows a (1 × 1) arrangement at 1 ML. An increased energy cost for adding water to the reconstructed CO_3 rows is revealed by DFT and explains these findings. Adsorbed water is identified to prefer an underlying unreconstructed (1 × 1) calcite(104) surface. Therefore, water lifts the (2 × 1) reconstruction of calcite(104) in the coverage regime between 0.5 and 1 ML in a progressive manner.

Results and discussion

The interaction of water with the unreconstructed (1 × 1) calcite(104) surface has intensively been studied.[11–18] It is now

[a] *Fachbereich Mathematik/Informatik/Physik, Universität Osnabrück, 49076 Osnabrück, Germany. E-mail: prahe@uos.de*
[b] *Faculty of Chemistry, Bielefeld University, 33615 Bielefeld, Germany*
[c] *Department of Applied Physics, Aalto University, Finland. E-mail: adam.foster@aalto.fi*
[d] *Nano Life Science Institute (WPI-NanoLSI), Kanazawa University, Kanazawa 920-1192, Japan*

† Electronic supplementary information (ESI) available: Materials and methods. Atomic shifts for {QS} water (Fig. S1), water row structures (Fig. S2), atomic shifts for {PR} water (Fig. S3), further geometries for water adsorption above 0.5 ML (Fig. S4), NEB calculations (Fig. S5), structure files for water/calcite(104) models (CIF files). See DOI: https://doi.org/10.1039/d3cp01408h

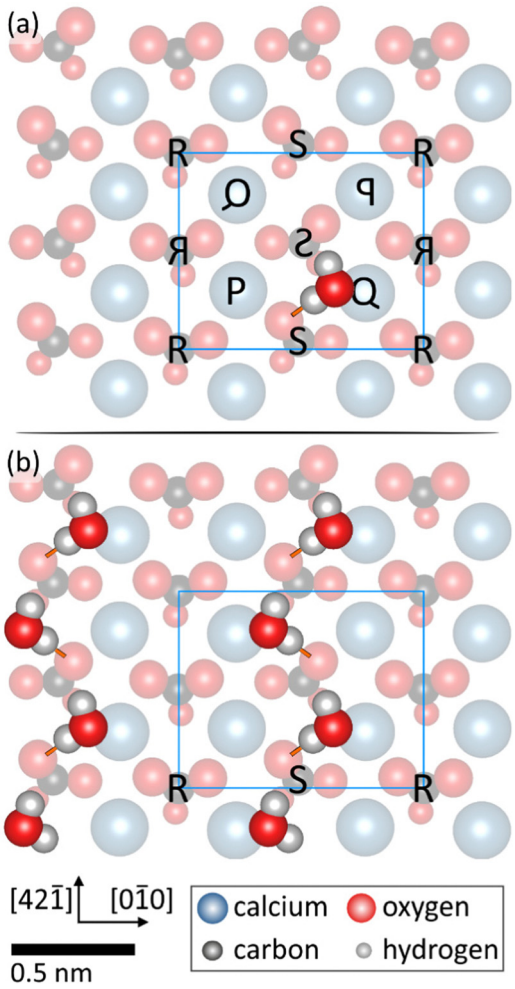

Fig. 1 DFT geometries of (a) a single QS water molecule and (b) 0.5 ML {QS} water coverage on calcite(104). The unit cell (blue rectangle) as well as the naming convention of the surface sites at the carbonate groups (R,S) and calcium atoms (P,Q) are included.

a general consensus that an adsorbed individual water molecule is located at an intermediate position between a surface Ca ion and CO_3 group and that the adsorption geometry is stabilised by both an oxygen–calcium bond between the water and calcite(104) surface, as well as by a hydrogen bond between one hydrogen atom of water and a protruding surface oxygen atom.[11] A total of four calcium ions are located within the top layer of the (2×1) unit cell of calcite(104). Consequently, a maximum of four water molecules bind to the surface per (2×1) surface unit cell in the first water layer as dictated by the oxygen–calcium bond; we identify this configuration as 1 monolayer (ML). However, there are effectively only two different adsorption positions within the (2×1) surface unit cell as the properties of the four positions within the unit cell are pairwise linked by the g symmetry element. The axes of glide reflection have previously been found to be located on the carbonate group rows.[5] Consequently, to account for both the surface reconstruction and symmetry, we denote the different calcium atom sites as P and Q, while their symmetry-equivalents are depicted by mirrored letters in Fig. 1(a), here denoted as P_m and Q_m. Accordingly, the different carbonate groups are named R and S with R_m and S_m being the symmetry-equivalent partners,[5] see also Fig. 1(a).

We perform DFT calculations with various positions and orientations of a single water molecule on a 4-layer slab consisting of two-by-two (2×1) unit cells and calculate the adsorption energy E_1 from

$$E_1 = (E_{\text{total},1} - E_{(2\times1)}) - E_{\text{water}}. \quad (1)$$

For this calculation, we use the total system energy $E_{\text{total},1}$ of a geometry-optimised water/calcite(104) surface model, the energy $E_{(2\times1)}$ of the (2×1) reconstructed water-free surface slab, and the energy E_{water} of a single water molecule in the gas phase. It has recently[5] been found that a geometry analysis in DFT, in particular the investigation of the (2×1) reconstruction, is dependent on the modelling of dispersion interactions. Therefore, in this work we use a similar simulation approach to that detailed in ref. 5 (see ESI† for further details on the methodology).

The lowest energy configuration with $E_1 = -0.98$ eV is shown in Fig. 1(a) where the water is positioned in-between a Q calcium ion and an unreconstructed S carbonate group row. Following the naming introduced above, we therefore refer to this binding configuration as QS water. This adsorption geometry is stabilised by an ionic O_{water}–Ca_{surf} (2.40 Å bond length) and a $H_{\text{water},1}$–O_{surf} hydrogen bond (1.80 Å bond length), the latter is indicated by an orange line in Fig. 1(a). Due to the large distance of 2.19 Å between the second hydrogen atom $H_{\text{water},2}$ and the nearby O_{surf}, we suspect that weak van der Waals attraction binds the second hydrogen atom to the surface. This adsorption geometry is in excellent agreement with previous studies of water on the unreconstructed calcite(104)–(1×1) surface.[11,12] We furthermore analyse the atomic shifts of the calcite surface atoms in comparison to the pristine (2×1) reconstruction (see ESI† Fig. S1(a)) and find only minor movements up to a maximum of about 12 pm. Thus, the large adsorption energy can also be seen as a result of only minor relaxation within the calcite(104) surface structure upon water adsorption.

For the coverage regime up to 0.5 ML, we calculate the energy per water molecule $E_{\{\text{QS}\},N}$ for a system containing N water molecules from

$$E_{\{\text{QS}\},N} = (E_{\text{total},N} - E_{(2\times1)})/N - E_{\text{water}}. \quad (2)$$

As the main result, we find that arranging {QS} (the set of QS and the symmetry-equivalent Q_mS_m positions) water molecules in rows along the [42$\bar{1}$] direction is the preferred adsorption geometry for coverage of 0.5 ML with the structure shown in Fig. 1(b) (see also ESI† Fig. S2 for further structures with higher adsorption energy per water molecule). In particular, DFT yields an adsorption energy per water of $E_{\{\text{QS}\},8} = -0.94$ eV for a system containing $N = 8$ water molecules, very close to $E_1 = -0.98$ eV for a single water molecule. Thus, the water adsorption up to a coverage of 0.5 ML is predominantly determined by the {QS} adsorption configuration with insignificant water-water

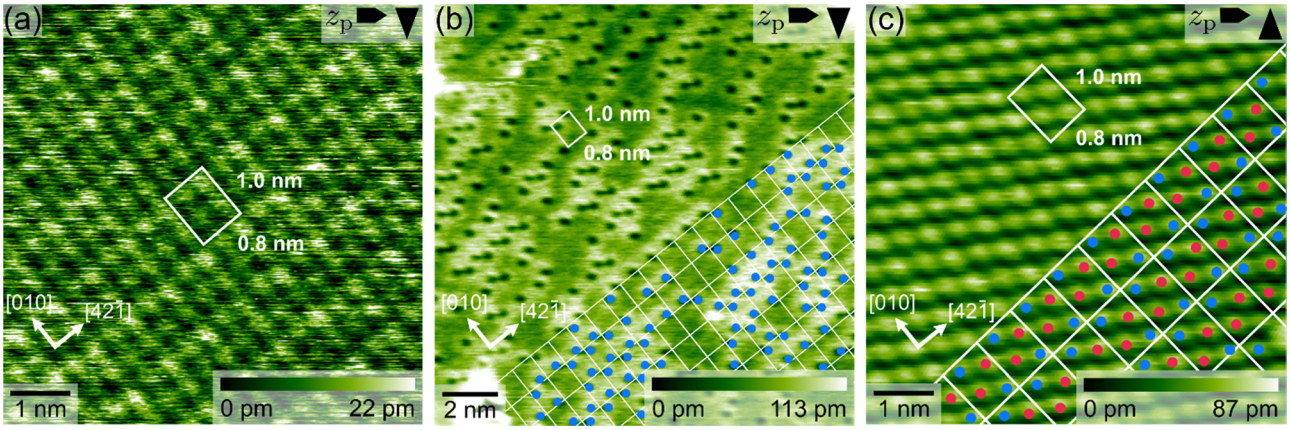

Fig. 2 NC-AFM image data of (a) the pristine calcite(104) surface, (b) calcite(104) with 0.26 ML water coverage, and (c) full water monolayer. Data have been corrected for thermal drift. A grid representing the (2 × 1) surface lattice is superimposed in (b) and (c). Blue and red dots represent the positions of {QS} and {PR} water, respectively. Images are acquired at (a) 300 K, (b and c) 140 K.

interactions as well as minor rearrangements of the underlying calcite(104) surface (see ESI† Fig. S1(b)).

Next, we compare the DFT findings at low coverage with experimental NC-AFM image data acquired in ultra-high vacuum at 140 K. For the NC-AFM experiments, a clean calcite(104) surface is first prepared by *in situ* cleaving and annealing in ultra-high vacuum. Second, water molecules are deposited on the cooled sample by dosing water through a leak valve (see ESI† for further details on the methodology). Fig. 2 presents results from a series with incremental water coverage. As apparent from Fig. 2(a), a (2 × 1) reconstruction and an asymmetric contrast within the unit cell along the [42$\bar{1}$] direction is imaged for a clean calcite(104) surface; the latter contrast is known to be caused by the probing tip.[5] Fig. 2(b) presents a micrograph of the calcite(104) surface after dosing about 0.038 Langmuir (L) of water onto a cooled surface. Single water molecules are identified as dark features and appear to be ordered along rows in [42$\bar{1}$] direction. A (2 × 1) surface lattice is superimposed to the drift-corrected[19,20] image and reveals that only one half of each (2 × 1) surface unit cell is filled by water molecules (blue dots in Fig. 2(b)). Most importantly, *the same half* of each unit cell is unoccupied up to a coverage of 0.5 ML. In contrast, when increasing the coverage to 1 ML (0.18 L, see Fig. 2(c)), no apparent differences between the (2 × 1) unit cell halves are apparent; instead, a stoichiometric (1 × 1) superstructure is suggested with all adsorption positions (blue and red dots) equally occupied.

The experimental observation of water occupying only one particular half of each (2 × 1) unit cell below 0.5 ML coverage suggests a lower adsorption energy per water for deposition at site {QS} compared to {PR} (the set containing the PR and the symmetry-equivalent P_mR_m positions) up to a coverage of 0.5 ML. In other words, the presence of the row structure in Fig. 1(b) and 2(b) can be seen as a direct consequence of the (2 × 1) reconstructed calcite(104) surface and, in particular, of an energetic difference between water adsorption at the {QS} and {PR} unit cell positions. It is noteworthy that the presence of two water adsorption sites with a difference in the water binding energy of about 0.3 eV has very recently been identified by temperature programmed desorption (TPD) experiments on calcite(104).[9] This difference would not be present on a (1 × 1) reconstructed surface. Instead, a random arrangement would be the expected structure for water deposition on an unreconstructed calcite(104)–(1 × 1) surface due to insignificant water–water interactions. Given a random impingement of water on the calcite(104) surface, we finally note that the transition from {PR} to {QS} sites appears to be possible at 140 K.

To unravel the mechanism behind the transition from the (2 × 1) to the (1 × 1) water structure in Fig. 2(b) and (c) at 0.26 ML and 1 ML, respectively, we perform geometry optimisation runs with DFT for a two-by-two (2 × 1) unit cell 4-layer slab containing N = 9 to 16 water molecules (corresponding to water coverage from about 0.56 to 1 ML). Surface models with progressively filling one [42$\bar{1}$] row are presented in Fig. 3(a) to (d). Two important observations are made when already adding a single water molecule to a {PR} position (Fig. 3(a), N = 9): First, we find that the adsorption energy $E_{\{PR\},9}$ for this water molecule as calculated from the difference

$$E_{\{PR\},9} = E_{total,9} - E_{total,8} - E_{water} = -0.71 \text{ eV} \quad (3)$$

is more positive than the adsorption energies for single {QS} water molecules (N = 1…8; $E_{\{QS\},N} < -0.9$ eV). This confirms the above suggestion that water adsorption at the {PR} positions is energetically less favourable than water adsorption at the {QS} positions. Second, the carbonate groups adjacent to this water molecule relax towards the unreconstructed bulk-like geometry with shifts as large as 59 pm (see ESI† Fig. S3(a)). Therefore, we explain the reduced adsorption energy for {PR} water by the additional energy required to reorient the water-adjacent surface carbonate groups from the reconstructed (2 × 1) orientation towards the bulk-like (1 × 1) geometry.

The results for adding further {PR} water molecules along [42$\bar{1}$] as shown in Fig. 3(b) to (d) substantiate this explanation as follows: we calculate the adsorption energy $E_{\{PR\},N}$ per {PR} water molecule from

$$E_{\{PR\},N} = (E_{total} - E_{\{QS\},8})/(N\text{-}8) - E_{water} \quad (4)$$

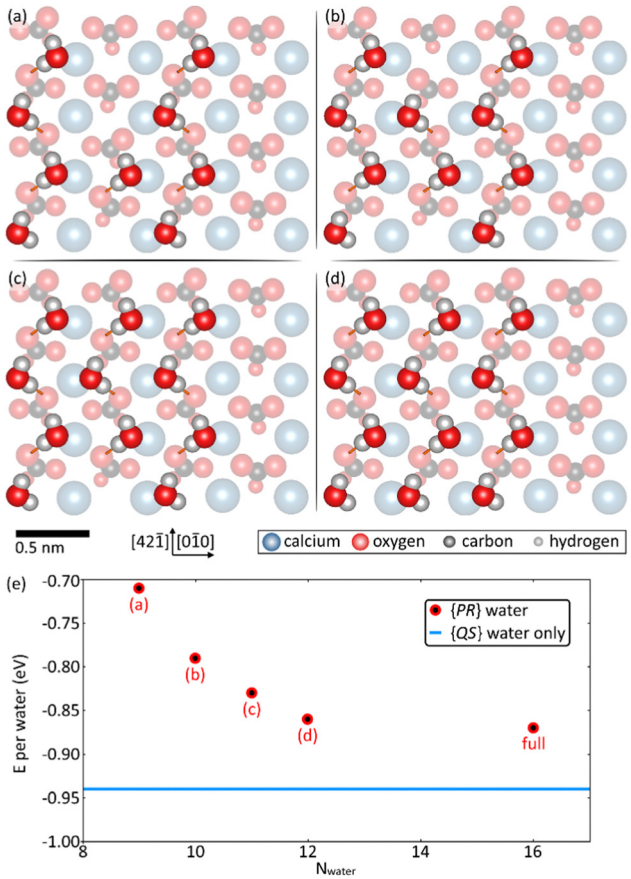

Fig. 3 (a–d) DFT-optimised geometries of filling one [42$\bar{1}$] row on calcite(104)-(2 × 1) with {PR}-type water. (e) Adsorption energy per water molecule for the different {PR} water–surface models ($E_{\{PR\},N}$, eqn (4), circles). The energy for {QS} water ($E_{\{QS\},8}$, eqn (2)) is indicated by a horizontal blue line. Geometry for 1 ML coverage (N = 16) is shown in ESI† Fig. S4(d).

using the energy $E_{\{QS\},8}$ for N = 8 water molecules at {QS} positions (see Fig. 1(b) and eqn (2)) as a reference. First, we analyse this energy for the cases N = 9 to N = 12 using the geometries shown in Fig. 3(a)–(d). For these models, where water is successively added along one [42$\bar{1}$] row, a clear trend of $E_{\{PR\},N}$ approaching $E_{\{QS\}}$ is apparent in Fig. 3(e). The energy change correlates with successively reduced displacement of the calcite(104) surface species (see ESI† Fig. S3). Second, we compare the case for N = 10 in Fig. 3(b) with a geometry of the two {PR} water molecules being separated by half a unit cell (see Fig. S4(a), ESI†), leading to the presence of two PR water adsorption sites. A binding energy of $E_{PR,10}$ = −0.77 eV, more positive than $E_{\{PR\},10}$ = −0.79 eV as in Fig. 3(b), is found and explained by the energy cost of rotating further surface carbonate groups. Third, the series in Fig. 3 is compared with two models for N = 10 and N = 12 that represent the case of adsorbing water along the [010] rows (see ESI† Fig. S4(b) and (c)). Adsorption energies of $E_{PR,10,b}$ = −0.72 eV and $E_{PR,12}$ = −0.79 eV are calculated for these two geometries, higher than the energies for the same number of water molecules when filling along a [42$\bar{1}$] row.

Our findings can directly be understood when considering the positions of the carbonate groups: The bond formation with each {PR} water molecule causes a rotation of the nearby *R*-row carbonate groups towards the bulk-like (1 × 1) geometry. Therefore, each additional water molecule adsorbed adjacent to already present {PR} water benefits from a calcite(104) surface structure already partly relaxed towards the (1 × 1) geometry. Thus, filling along the [42$\bar{1}$] direction is beneficial, while water adsorption in rows along the [010] direction includes an additional energy cost for rotating more carbonate groups towards the (1 × 1) surface geometry. Due to the finite slab size, the energy cost for carbonate group reorientation is smallest at N = 12 within this series.

The increased adsorption strength upon filling the {PR} positions along the [42$\bar{1}$] direction explains the formation of islands despite the absence of direct water–water interaction. These islands can indeed be observed experimentally when imaging the water structure at coverage of about 0.67 ML, see Fig. 4: the NC-AFM image data reveal dense areas in addition to the half-filled row structure that dominates the water adsorption up to 0.5 ML coverage. In the imaged water structure, a substrate-mediated attraction between neighbouring water molecules adsorbed next to a reconstructed [42$\bar{1}$] carbonate group row is generated by the reorientation of the surface carbonate groups as analysed by DFT before. As a consequence, the {PR} positions are not filled randomly, but the water molecules appear to diffuse, likely along the [42$\bar{1}$] rows *via* the {PR} positions, until nucleation occurs. From nudged elastic band (NEB) calculations we find barriers for single PR water molecule diffusion of the order of 0.5 to 0.6 eV (see ESI† Fig. S5), with a smaller barrier for the system shown in Fig. 3(a) (N = 9) than for the system in Fig. 3(b) (N = 10).

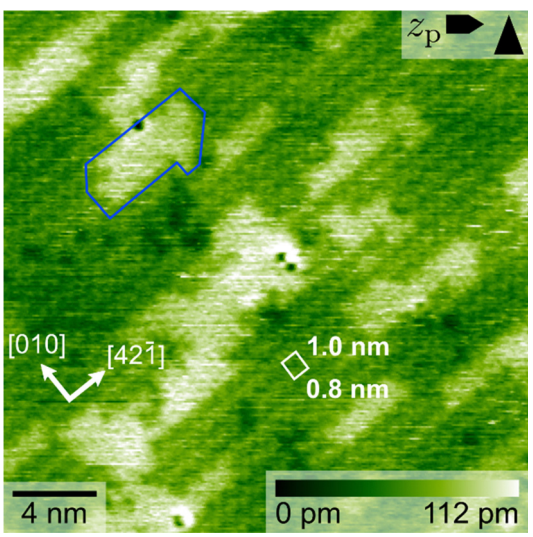

Fig. 4 NC-AFM image acquired at 140 K after deposition of 0.12 L water. The formation of dense patches in addition to the {QS} row water structure is apparent (one example marked by a blue box). With a coverage of 2/4 (4/4) of water molecules within a (2 × 1) unit cell in the striped (dense) phase, the total water coverage in the image is 0.67 ML.

Conclusions

The water adsorption properties on calcite(104) are strongly influenced by the (2 × 1) reconstruction in the coverage regime of up to 1 ML. Both NC-AFM and DFT find a clear preference of water adsorption at the {QS} positions for coverage up to 0.5 ML and row structures with only half-filled (2 × 1) surface unit cells are observed in this regime by NC-AFM. The key mechanism defining the adsorption properties above 0.5 ML is the reorientation of the calcite surface adjacent to the water molecules at the {PR} positions. This reorientation of the carbonate groups and calcium atoms leads to a cost in the adsorption energy, a preference for water nucleation, as well as the formation of islands. Given the absence of significant water–water interactions, the island formation can be understood to be mediated by the substrate. As a consequence, the underlying calcite(104)–(2 × 1) surface reconstruction is lifted and the surface starts to express areas of an unreconstructed (1 × 1) termination at water coverage above 0.5 ML.

The difference in adsorption energy at the two different adsorption sites suggest a measurable impact on the various processes involving the calcite(104) surface. Therefore, our work demonstrates the significant influence of the (2 × 1) reconstruction of calcite(104) on the adsorption structure of water, leading to a characteristic sequence of superstructures and the formation of substrate-mediated islands.

Author contributions

JH and SA performed the experiments under supervision of RB. JH, SA and TD analysed the data. TD provided software for the data analysis. YSR and ASF performed the DFT calculations. TD, RB, AK, and PR contributed to the data analysis and interpretation. RB, AK, and PR conceptualised the investigation. ASF, AK, and PR acquired funding. PR wrote the initial draft. All authors contributed to writing the manuscript and discussing the results.

Conflicts of interest

There are no conflicts to declare.

Acknowledgements

PR and AK gratefully acknowledge financial support from the German research foundation (DFG) *via* grants RA2832/1-1, RA2832/1-2, RA2832/2-1, and KU1980/11-1. The University of Osnabrück supported this study *via* the Innovationspool. YSR and ASF were supported by the World Premier International Research Center Initiative (WPI), MEXT, Japan and by the Academy of Finland (Project No. 314862).

Notes and references

1 G. E. Brown and G. Calas, *Geochem. Perspect.*, 2012, **1**, 483–742.
2 G. E. Brown, *Science*, 2001, **294**, 67–70.
3 A. Putnis, *Science*, 2014, **343**, 1441–1442.
4 J. Aizenberg, A. Tkachenko, S. Weiner, L. Addadi and G. Hendler, *Nature*, 2001, **412**, 819.
5 J. Heggemann, Y. S. Ranawat, O. Krejčí, A. S. Foster and P. Rahe, *J. Phys. Chem. Lett.*, 2023, **14**, 1983–1989.
6 N. H. de Leeuw and S. C. Parker, *J. Phys. Chem. B*, 1998, **102**, 2914–2922.
7 J. Schütte, P. Rahe, L. Tröger, S. Rode, R. Bechstein, M. Reichling and A. Kühnle, *Langmuir*, 2010, **26**, 8295–8300.
8 S. L. S. Stipp, *Geochim. Cosmochim. Acta*, 1999, **63**, 3121–3131.
9 T. Dickbreder, D. Lautner, A. Köhler, L. Klausfering, R. Bechstein and A. Kühnle, *Phys. Chem. Chem. Phys.*, 2023, **25**, 12694.
10 H. Söngen, C. Marutschke, P. Spijker, E. Holmgren, I. Hermes, R. Bechstein, S. Klassen, J. Tracey, A. S. Foster and A. Kühnle, *Langmuir*, 2017, **33**, 125–129.
11 J. S. Lardge, D. M. Duffy and M. J. Gillan, *J. Phys. Chem. C*, 2009, **113**, 7207–7212.
12 E. Ataman, M. P. Andersson, M. Ceccato, N. Bovet and S. L. S. Stipp, *J. Phys. Chem. C*, 2016, **120**, 16586–16596.
13 N. Laanait, E. B. R. Callagon, Z. Zhang, N. C. Sturchio, S. S. Lee and P. Fenter, *Science*, 2015, **349**, 1330–1334.
14 K. Umeda, K. Kobayashi, T. Minato and H. Yamada, *Phys. Rev. Lett.*, 2019, **122**, 116001.
15 H. Söngen, B. Reischl, K. Miyata, R. Bechstein, P. Raiteri, A. L. Rohl, J. D. Gale, T. Fukuma and A. Kühnle, *Phys. Rev. Lett.*, 2018, **120**, 116101.
16 M. De La Pierre, P. Raiteri and J. D. Gale, *Cryst. Growth Des.*, 2016, **16**, 5907–5914.
17 P. Fenter, S. Kerisit, P. Raiteri and J. D. Gale, *J. Phys. Chem. C*, 2013, **117**, 5028–5042.
18 J. S. Lardge, D. M. Duffy, M. J. Gillan and M. Watkins, *J. Phys. Chem. C*, 2010, **114**, 2664–2668.
19 P. Rahe, R. Bechstein and A. Kühnle, *J. Vac. Sci. Technol., B*, 2010, **28**, C4E31.
20 T. Dickbreder, F. Sabath, L. Höltkemeier, R. Bechstein and A. Kühnle, *submitted*, 2023.